Eur. Phys. J. C 54, 577–581 (2008)
DOI 10.1140/epjc/s10052-008-0554-1

THE EUROPEAN PHYSICAL JOURNAL C

Regular Article – Theoretical Physics

Midrapidity production of secondaries in pp collisions at RHIC and LHC energies in the quark–gluon string model

G.H. Arakelyan[1,a], C. Merino[2,b], C. Pajares[2,c], Y.M. Shabelski[3,d]

[1] Yerevan Physics Institute, Armenia
[2] Departamento de Física de Partículas, Facultade de Física, and Instituto Galego de Altas Enerxías (IGAE), Universidade de Santiago de Compostela, Galicia, Spain
[3] Petersburg Nuclear Physics Institute, Gatchina, St. Petersburg, 188350, Russia

Received: 20 September 2007 /
Published online: 28 February 2008 –

Abstract. We consider the phenomenological implications of the assumption that baryons are systems of three quarks connected through a gluon string junction. The transfer of baryon number in rapidity space due to the string junction propagation is considered in detail. At high energies this process leads to a significant effect on the net baryon production in hN collisions at midrapidities. The numerical results for midrapidity inclusive densities of different secondaries in the framework of the quark–gluon string model are in reasonable agreement with the experimental data. One universal value, $\lambda \simeq 0.25$, for the strangeness suppression parameter correctly describes the yield ratios of Λ/p, Ξ/Λ, and Ω/Ξ. The predictions for pp collisions at LHC energies are also presented.

PACS. 25.75.Dw

1 Introduction

The quark–gluon string model (QGSM) and the dual parton model (DPM) are based on dual topological unitarization (DTU), and they describe quite reasonably many features of high energy production processes in both hadron–nucleon and hadron–nucleus collisions [1–8]. High energy interactions are considered as taking place via the exchange of one or several pomerons, all elastic and inelastic processes resulting from cutting through or between pomerons [9]. Inclusive spectra of hadrons are related to the corresponding fragmentation functions of quarks and diquarks, which are constructed using the reggeon counting rules [10, 11].

In string models, baryons are considered as configurations consisting of three connected strings (related to three valence quarks) called a string junction (SJ) [12–17]. In the processes of secondary production the SJ diffusion in rapidity space leads to significant differences in the yields of baryons and antibaryons in the midrapidity region even at very high energies [18].

A quantitative theoretical description of baryon number transfer via the SJ mechanism was suggested in the nineties. The later experimentally observed $p/\bar{p}$ asymmetry at HERA energies was predicted [19, 20], and in [21, 22] it was noted that the $p/\bar{p}$ asymmetry measured at HERA can be obtained by simple extrapolation of the ISR data.

Important results on the baryon number transfer due to SJ diffusion in rapidity space were obtained in [23, 24] and subsequent papers [25–38].

In the present paper, we calculate the inclusive densities of different secondaries and compare them with recent RHIC data [39] for pp collisions at $\sqrt{s} = 200$ GeV. The predictions for secondary production at LHC energies are also given.

2 Baryon as $3q$ + SJ system

In QCD, the hadrons are composite bound state configurations built up from the quark $\psi_i(x)$, $i = 1, \ldots, N_c$, and gluon $G^\mu_a(x)$, $a = 1, \ldots, N_c^2 - 1$, fields. In the string models the color part of a baryon wave function reads as follows (see Fig. 1) [12, 16]:

$$B = \psi_i(x_1)\psi_j(x_2)\psi_k(x_3)J^{ijk}(x_1, x_2, x_3, x), \tag{1}$$

$$J^{ijk}(x_1, x_2, x_3, x) = \Phi^i_{i'}(x_1, x)\Phi^j_{j'}(x_2, x)\Phi^k_{k'}(x_3, x)\epsilon^{i'j'k'}, \tag{2}$$

$$\Phi^{i'}_i(x_1, x) = \left[T \exp\left(g \int_{P(x_1,x)} A_\mu(z)\,\mathrm{d}z^\mu\right)\right]^{i'}_i, \tag{3}$$

[a] e-mail: argev@mail.yerphi.am
[b] e-mail: merino@fpaxp1.usc.es
[c] e-mail: pajares@fpaxp1.usc.es
[d] e-mail: shabelsk@thd.pnpi.spb.ru

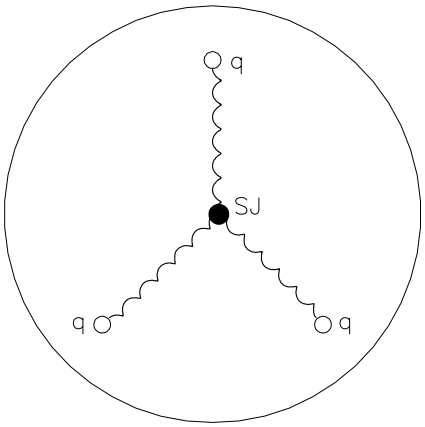

Fig. 1. Composite structure of a baryon in string models. Quarks are shown by *open points*

where x_1, x_2, x_3 and x are the coordinates of the valence quarks and SJ, respectively, and $P(x_1, x)$ represents a path from x_1 to x that looks like an open string with ends at x_1 and x.

The baryon wave function in (3) can be defined as a star (or Y) configuration. The Y baryon structure is supported by lattice calculations [40].

This picture leads to some general phenomenological predictions. In particular, it opens room for exotic states, such as the multiquark bound states, 4-quark mesons and pentaquarks [16, 41–43]. In the case of inclusive reactions the baryon number transfer to large rapidity distances in hadron–nucleon and hadron–nucleus reactions can be explained by SJ diffusion.

3 Inclusive spectra of secondary hadrons in the quark–gluon string model

To perform more quantitative predictions a model for multiparticle production has to be adopted. In the present paper we have used the QGSM for the numerical calculations. As was mentioned above, high energy hadron–nucleon collisions are considered in the QGSM as going via the exchange of one or several pomerons. Each pomeron corresponds to a cylindrical diagram (see Fig. 2a), and thus, when cutting a pomeron, two showers of secondaries are produced as is shown in Fig. 2b. The inclusive spectrum of a secondary hadron h is then determined by the convolution of the diquark, the valence quark, and the sea quark distributions $u(x, n)$ in the incident particles with the fragmentation functions $G^h(z)$ of quarks and diquarks into the secondary hadron h. Both the diquark and the quark distribution functions depend on the number n of cut pomerons in the considered diagram.

For a nucleon target, the inclusive spectrum of a secondary hadron h has the form [1, 2]

$$\frac{\mathrm{d}n}{\mathrm{d}y} = \frac{x_E}{\sigma_{\mathrm{inel}}}\frac{\mathrm{d}\sigma}{\mathrm{d}x_{\mathrm{F}}} = \sum_{n=1}^{\infty} w_n \phi_n^h(x)\,, \tag{4}$$

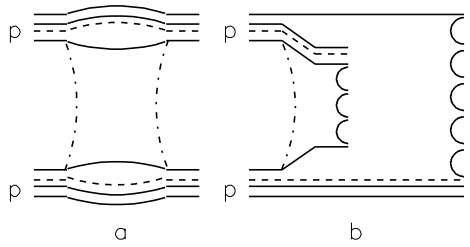

Fig. 2. Cylindrical diagram corresponding to the one-pomeron exchange contribution to elastic *pp* scattering (**a**) and the cut of this diagram which determines the contribution to the inelastic *pp* cross section (**b**). Quarks are shown by *solid curves* and SJ by *dashed curves*

where the functions $\phi_n^h(x)$ determine the contribution of diagrams with n cut pomerons, and w_n is the relative weight of this diagram. Here we neglect the contribution of diffraction dissociation processes, which is very small in the midrapidity region.

For *pp* collisions

$$\phi_{pp}^h(x) = f_{qq}^h(x_+, n) f_q^h(x_-, n) + f_q^h(x_+, n) f_{qq}^h(x_-, n) + 2(n-1) f_s^h(x_+, n) f_s^h(x_-, n)\,, \tag{5}$$

$$x_\pm = \frac{1}{2}\left[\sqrt{4m_{\mathrm{T}}^2/s + x^2} \pm x\right]\,, \tag{6}$$

where f_{qq}, f_q, and f_s correspond to the contributions of diquarks, valence quarks, and sea quarks, respectively.

These functions are determined by the convolution of the diquark and quark distributions with the fragmentation functions, e.g.

$$f_q^h(x_+, n) = \int_{x_+}^1 u_q(x_1, n) G_q^h(x_+/x_1)\,\mathrm{d}x_1\,. \tag{7}$$

The diquark and quark distributions, which are normalized to unity, as well as the fragmentation functions are determined by Regge intercepts [10, 11].

At very high energies both x_+ and x_- are negligibly small in the midrapidity region. In this case all fragmentation functions, which are usually written [10, 11] $G_q^h(z) = a_h(1-z)^\beta$, are constants,

$$G_q^h(x_+/x_1) = a_h\,, \tag{8}$$

and lead, in agreement with [44], to

$$\frac{\mathrm{d}n}{\mathrm{d}y} = g_h(s/s_0)^{\alpha_P(0)-1} \sim a_h^2(s/s_0)^{\alpha_P(0)-1}\,, \tag{9}$$

corresponding to the only one-pomeron exchange diagram in Fig. 3, which is the only diagram contributing to the inclusive density in the central region (AGK theorem [9]). The intercept of the supercritical pomeron, $\alpha_P(0) = 1 + \Delta$, $\Delta = 0.139$ [8], is used in the numerical calculations.

The diagram in Fig. 3 predicts equal inclusive yields for each particle and its antiparticle. However, some corrections to the spectra of secondary baryons appear for processes that present SJ diffusion in rapidity space. Although these

corrections would become negligible at energies asymptotically high, they result in a significant difference of the baryon and antibaryon yields in the midrapidity region for the currently available energy range. Moreover, this difference vanishes only very slowly when the energy increases.

According to [23, 24], we consider three different possibilities to obtain the net baryon charge. The first one is the fragmentation of the diquark giving rise to a leading baryon (Fig. 4a). A second possibility is to produce a leading meson in the first break-up of the string and a baryon in the subsequent break-up [10, 11, 45] (Fig. 4b). In these two cases baryon number transfer is possible only for short distances in rapidity. In the third case shown in Fig. 4c both initial valence quarks recombine with sea antiquarks into mesons M and a secondary baryon is formed by the SJ together with three sea quarks.

The corresponding fragmentation functions for the secondary baryon B production can be written as follows [23, 24]:

$$G^B_{qq}(z) = a_N v_{qq} z^{2.5}\,, \tag{10}$$

$$G^B_{qs}(z) = a_N v_{qs} z^2 (1-z)\,, \tag{11}$$

$$G^B_{ss}(z) = a_N \varepsilon v_{ss} z^{1-\alpha_{\rm SJ}} (1-z)^2 \tag{12}$$

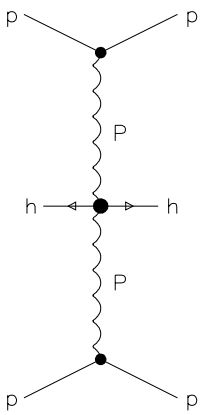

Fig. 3. One-pomeron pole diagram determining secondary hadron h production

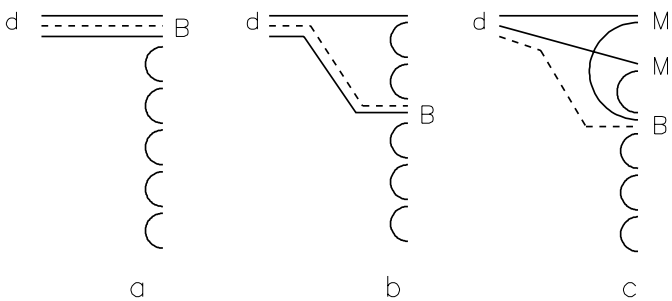

Fig. 4. QGSM diagrams describing secondary baryon B production by diquark d: initial SJ together with two valence quarks and one sea quark (**a**), initial SJ together with one valence quark and two sea quarks (**b**), and initial SJ together with three sea quarks (**c**)

for the processes shown in Fig. 4a, b, and c, respectively and where a_N is the normalization parameter; v_{qq}, v_{qs} and v_{ss} are the relative probabilities for different baryons production that can be found by simple quark combinatorics [46, 47]. The fraction z of the incident baryon energy carried by the secondary baryon decreases from Fig. 4a to c, whereas the mean rapidity gap between the incident and secondary baryon increases. The first two processes cannot contribute to the inclusive spectra in the central region, but the third contribution is essential if the value of the intercept of the SJ exchange Regge trajectory, $\alpha_{\rm SJ}$, is close to unity. The contribution of the graph in Fig. 4c has a coefficient ε that determines the small probability of such baryon number transfer.

In [23, 24] the value $\alpha_{\rm SJ} = 0.5$ was used. However, for such a value of $\alpha_{\rm SJ}$, different values of ε were needed for the correct description of the experimental data at moderate and high energies. This problem was solved in [25, 26], where it was shown with the help of more recent experimental data that all the data can be described with the parameter values

$$\alpha_{\rm SJ} = 0.9 \quad \text{and} \quad \varepsilon = 0.024\,. \tag{13}$$

It is necessary to note that the process shown in Fig. 4c can be realized very naturally in the quark combinatoric approach [46] with the specified probabilities of a valence quark recombination (fusion) with sea quarks and antiquarks.

4 Comparison with the experimental data

The probabilities w_n in (4) are calculated in the framework of reggeon theory [1, 2]. The normalization constants a_π (pion production), a_K (kaon production), $a_{\bar N}$ ($B\bar B$ pair production), and a_N (baryon production due to SJ diffusion) were determined [1–4, 8] from the experimental data at fixed target energies, where the fragmentation functions are not constants. The values of these parameters have not been modified for the present calculations, while the values of the corresponding constants for hyperons have been calculated by quark combinatorics [46, 47]. For sea quarks we have

$$\begin{aligned} p : n : \Lambda + \Sigma : \Xi^0 : \Xi^- : \Omega \\ = 4L^3 : 4L^3 : 12L^2 S : 3LS^2 : 3LS^2 : S^3\,. \end{aligned} \tag{14}$$

The ratio S/L determines the strange suppression factor, and $2L + S = 1$. Usually in soft processes the ratio $\lambda = S/L$ is assumed to be 0.2–0.35. Inside this region it should be considered as a free parameter and in the numerical calculation we have used the value $\lambda = S/L = 0.25$, which leads to the best agreement with the data [39].

The calculated inclusive densities of different secondaries at RHIC, $\sqrt{s} = 200\,\text{GeV}$, and LHC, $\sqrt{s} = 14\,\text{TeV}$, energies are presented in Table 1, where one can see that the agreement of the QGSM calculations with RHIC experimental data [39] is reasonably good.

Table 1. The QGSM results for midrapidity yields $\mathrm{d}n/\mathrm{d}y$ ($|y| < 0.5$) for different secondaries at RHIC and LHC energies. The results for $\varepsilon = 0.024$ are presented only when different from the case $\varepsilon = 0$. The agreement of the QGSM calculations with RHIC experimental data [39] is reasonably good

Particle	RHIC ($\sqrt{s} = 200$ GeV)			LHC ($\sqrt{s} = 14$ TeV)	
	$\varepsilon = 0$	$\varepsilon = 0.024$	Experiment [39]	$\varepsilon = 0$	$\varepsilon = 0.024$
π^+	1.27			2.54	
π^-	1.25			2.54	
K^+	0.13		0.14 ± 0.01	0.25	
K^-	0.12		0.14 ± 0.01	0.25	
p	0.0755	0.0861		0.177	0.184
$\overline{p}$	0.0707			0.177	
Λ	0.0328	0.0381	0.0385 ± 0.0035	0.087	0.0906
$\overline{\Lambda}$	0.0304		0.0351 ± 0.0032	0.0867	
Ξ^-	0.00306	0.00359	0.0026 ± 0.0009	0.0108	0.0112
$\overline{\Xi}^+$	0.00298		0.0029 ± 0.001	0.0108	
Ω^-	0.00020	0.00025	*	0.000902	0.000934
$\overline{\Omega}^+$	0.00020		*	0.000902	

* $\mathrm{d}n/\mathrm{d}y(\Omega^- + \overline{\Omega}^+) = 0.00034 \pm 0.00019$

The ratios of $\bar{p}/p$ production in pp interactions at $\sqrt{s} = 200$ GeV as functions of the rapidity have been calculated in the QGSM with the same parameters as used in [36–38], and they are in reasonable agreement with the experimental data [48, 49] if the SJ contribution with $\varepsilon = 0.024$ is included, while the disagreement is evident for the calculation without SJ contribution (i.e. with $\varepsilon = 0$). It is necessary to note that at asymptotically high energies the ratio $\bar{p}/p$ in the central region is expected to be equal to the unity, so any deviation of the $\bar{p}/p$ ratio from unity has to be explained in particular. One can see in Table 1 that at the RHIC energies the SJ contribution makes the deviation of $\bar{p}p$ from unity in the midrapidity region about three times larger than in the calculation without SJ contribution.

The QGSM predicts the deviation of $\bar{p}p$ ratios from unity due to the SJ contribution on the level of 3%–4% accuracy even at the LHC energy. Without SJ contribution these ratios are exactly equal to unity.

The QGSM calculations [25, 26] predict practically equal values of the $\bar{B}/B$ ratios in the midrapidity region independently on baryon strangeness, which is qualitatively confirmed by the RHIC data on Au–Au collisions [50]. In the case of $\Omega/\bar{\Omega}$ production in pp collisions we obtain a non-zero asymmetry (i.e. more Ω than $\bar{\Omega}$), which is necessarily absent in the naive quark model or in all recombination models, since both Ω and $\bar{\Omega}$ have no common valence quarks with the incident particles.

In Fig. 5 we reproduce the experimental data on the ratios of the yields of different secondaries [39] together with our calculations. Agreement is good with the only exception of the point of the $\bar{p}/\pi^-$ ratio. From the comparison of our results with the experimental data presented in Table 1 and Fig. 5, we can conclude that the universal parameter $\lambda = 0.25$ describes the ratios of Λ/p, Ξ/Λ, and Ω/Ξ production in a reasonable way.

5 Conclusion

We discuss the role of string junction diffusion in baryon charge transfer over large rapidity distances for the cases of pp collisions at RHIC and LHC energies. The inclusion of the SJ contribution provides a reasonable description of the main bulk of existing experimental data. The calculations of the baryon/antibaryon yields and asymmetries without SJ contribution [23–26] clearly diverge for most of the experimental data where this contribution should

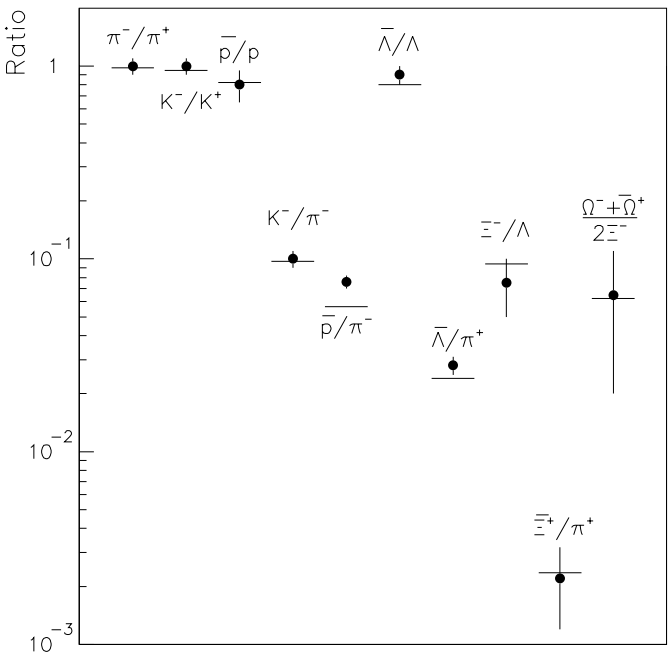

Fig. 5. Ratios of different secondaries produced in midrapidity region in pp collisions at $\sqrt{s} = 200$ GeV. *Short horizontal solid lines* show the results of the QGSM calculations

be important. Similar results for antibaryon to baryon production ratios at RHIC and LHC energies are presented in [52, 53]. These are obtained in the framework of DPMJET-III Monte Carlo. Some numerical difference with our results comes mainly from the different values of the α_{SJ} parameter.

Acknowledgements. We are grateful to F. Bopp for useful discussions. This paper was supported by Ministerio Educación y Ciencia of Spain under project FPA 2005-01963 and by Xunta de Galicia and, in part, by grants RFBR-07-02-00023 and RSGSS-1124.2003.2.

References

1. A.B. Kaidalov, K.A. Ter-Martirosyan, Yad. Fiz. **39**, 1545 (1984)
2. A.B. Kaidalov, K.A. Ter-Martirosyan, Yad. Fiz. **40**, 211 (1984)
3. A.B. Kaidalov, O.I. Piskounova, Yad. Fiz. **41**, 1278 (1985)
4. A.B. Kaidalov, O.I. Piskounova, Z. Phys. C **30**, 145 (1986)
5. A. Capella, U. Sukhatme, C.I. Tan, J. Tran Thanh Van, Phys. Rep. **236**, 225 (1994)
6. A. Capella, J. Tran Thanh Van, Z. Phys. C **10**, 249 (1981)
7. A.B. Kaidalov, K.A. Ter-Martirosyan, Y.M. Shabelski, Yad. Fiz. **43**, 1282 (1986)
8. Y.M. Shabelski, Yad. Fiz. **44**, 186 (1986)
9. V.A. Abramovsky, V.N. Gribov, O.V. Kancheli, Yad. Fiz. **18**, 595 (1973)
10. A.B. Kaidalov, Sov. J. Nucl. Phys. **45**, 902 (1987)
11. A.B. Kaidalov, Yad. Fiz. **43**, 1282 (1986)
12. X. Artru, Nucl. Phys. B **85**, 442 (1975)
13. M. Imachi, S. Otsuki, F. Toyoda, Prog. Theor. Phys. **52**, 346 (1974)
14. M. Imachi, S. Otsuki, F. Toyoda, Prog. Theor. Phys. **54**, 280 (1976)
15. M. Imachi, S. Otsuki, F. Toyoda, Prog. Theor. Phys. **55**, 551 (1976)
16. G.C. Rossi, G. Veneziano, Nucl. Phys. B **123**, 507 (1977)
17. D. Kharzeev, Phys. Lett. B **378**, 238 (1996)
18. Y.M. Shabelski, hep-ph/0211387
19. B.Z. Kopeliovich, B. Povh, Z. Phys. C **75**, 693 (1997)
20. B.Z. Kopeliovich, B. Povh, Phys. Lett. B **446**, 321 (1999)
21. F. Bopp, hep-ph/0002190
22. F. Bopp, hep-ph/0007229
23. G.H. Arakelyan, A. Capella, A.B. Kaidalov, Y.M. Shabelski, Eur. Phys. J. C **26**, 81 (2002)
24. G.H. Arakelyan, A. Capella, A.B. Kaidalov, Y.M. Shabelski, hep-ph/0103337
25. F. Bopp, Y.M. Shabelski, Yad. Fiz. **68**, 2155 (2005)
26. F. Bopp, Y.M. Shabelski, hep-ph/0406158
27. G.H. Arakelyan, C. Merino, Y.M. Shabelski, Yad. Fiz. **69**, 911 (2006)
28. G.H. Arakelyan, C. Merino, Y.M. Shabelski, hep-ph/0505100
29. G.H. Arakelyan, C. Merino, Y.M. Shabelski, Phys. Atom. Nucl. **70**, 1110 (2007)
30. G.H. Arakelyan, C. Merino, Y.M. Shabelski, hep-ph/0604103
31. G.H. Arakelyan, C. Merino, Y.M. Shabelski, Eur. Phys. J. A **31**, 519 (2007)
32. G.H. Arakelyan, C. Merino, Y.M. Shabelski, hep-ph/0610264
33. G.H. Arakelyan, C. Merino, Y.M. Shabelski, hep-ph/0707.1491
34. O.I. Piskounova, Phys. Atom. Nucl. **70**, 1110 (2007)
35. O.I. Piskounova, hep-ph/0604157
36. F. Bopp, Y.M. Shabelski, Eur. Phys. J. A **28**, 237 (2006)
37. F. Bopp, Y.M. Shabelski, hep-ph/0603193
38. Y.M. Shabelski, hep-ph/0705.0947
39. STAR Collaboration, B.I. Abelev et al., nucl-ex/0607033
40. V.G. Bornyanov et al., Usp. Fiz. Nauk. **174**, 19 (2004)
41. D. Diakonov, V. Petrov, M. Polyakov, Z. Phys. A **359**, 305 (1997)
42. M.G. Ryskin, Y.M. Shabelski, Eur. Phys. J. C **50**, 81 (2007)
43. M.G. Ryskin, Y.M. Shabelski, hep-ph/0609222
44. V.A. Abramovsky, O.V. Kancheli, I.D. Mandzhavidze, Yad. Fiz. **13**, 1102 (1971)
45. A. Capella, B.Z. Kopeliovich, Phys. Lett. B **381**, 325 (1996)
46. V.V. Anisovich, V.M. Shekhter, Nucl. Phys. B **55**, 455 (1973)
47. A. Capella, C.-A. Salgado, Phys. Rev. C **60**, 054 906 (1999)
48. BRAHMS Collaboration, I.G. Bearden et al., Phys. Lett. B **607**, 42 (2005)
49. BRAHMS Collaboration, I.G. Bearden et al., nucl-ex/0409002
50. B. Muller, J.L. Nagle, nucl-th/0602029
51. H. Noda, Prog. Theor. Phys. **68**, 1406 (1982)
52. F. Bopp, R. Engel, J. Ranft, S. Roesler, hep-ph/0505035
53. F. Bopp, R. Engel, J. Ranft, S. Roesler, hep-ph/0706.3870